

DISCOVERY OF GAMMA-RAY ORBITAL MODULATION IN THE BLACK WIDOW PSR J1311–3430

YI XING AND ZHONGXIANG WANG

Key Laboratory for Research in Galaxies and Cosmology, Shanghai Astronomical Observatory,
 Chinese Academy of Sciences, 80 Nandan Road, Shanghai 200030, China

Draft version January 27, 2022

ABSTRACT

We report our discovery of orbitally modulated γ -ray emission from the black widow system PSR J1311–3430. We analyze the *Fermi* Large Area Telescope data during the offpulse phase interval of the pulsar, and find the orbital modulation signal at a $\sim 3\sigma$ confidence level. Further spectral analysis shows no significant differences for the spectra obtained during the bright and faint orbital phase ranges. A simple sinusoid-like function can describe the modulation. Given these properties, we suggest that the intrabinary γ -ray emission arises from the region close to the companion and the modulation is caused by the occultation of the emitting region by the companion, similar to that is seen in the transitional millisecond pulsar binary (MSP) PSR J1023+0038. Considering the X-ray detection of intrabinary shock emission from eclipsing MSP binaries recently reported, this discovery further suggests the general existence of intrabinary γ -ray emission from them.

Subject headings: binaries: close — pulsars: individual (PSR J1311–3430) — gamma rays: stars

1. INTRODUCTION

Millisecond pulsars (MSPs) are widely accepted to be old neutron stars that were spun up through mass accretion from the companions when they were at the low-mass X-ray binary phase (Alpar et al. 1982; Radhakrishnan & Srinivasan 1982). Not surprisingly, $>60\%$ known MSPs are in binaries (e.g., Manchester et al. 2005). A sub-class of them, so-called ‘black widow’ pulsar systems (Fruchter et al. 1988), have very low-mass, $\sim 0.02 M_{\odot}$ companions. To form isolated MSPs, one possible channel is through ablation of the companions by the pulsar wind. This possibility likely occurs in the black widows since they are eclipsing systems at radio frequencies, indicating the interaction between the pulsar wind and the companions. X-ray observations of them revealed orbital flux variations, also supporting the presence of the intrabinary interaction (Huang et al. 2012; Gentile et al. 2014). In addition, recent extensive studies of the so-called ‘redback’ systems (Roberts 2013) have provided clear evidence for the interaction. These redbacks are also eclipsing MSP binaries, but contain relative massive, $\sim 0.1\text{--}0.6 M_{\odot}$ companions. X-ray observations of the prototypical redback PSR J1023+0038 detected significant orbital flux variations (Archibald et al. 2010; Bogdanov et al. 2011), and the variations can be explained by the existence of an intrabinary shock region (Bogdanov et al. 2011). Similar features were also clearly seen in the redback XSS J12270–4859 (Bogdanov et al. 2014 and references therein).

Owing to its all-sky monitoring and high sensitivity capabilities, the *Fermi* Gamma-ray Space Telescope, launched in 2008, has greatly improved our studies of pulsars. For MSPs, more than six-fold black widows and redbacks have been discovered with the help of *Fermi* (e.g., Roberts 2013). At *Fermi*’s 100 MeV to 300 GeV energy range, marginal evidence for the intrabinary interaction in the eclipsing systems has also been seen. For the first discovered black widow PSR B1957+20

(Fruchter et al. 1988), an orbital modulation signal was detected at a $\sim 2.3\sigma$ confidence level (Wu et al. 2012). In addition, possible signals were also reported for XSS J12270–4859 (Xing & Wang 2014) and a candidate redback 2FGL J0523.3–2530 (Xing et al. 2014). Theoretical studies have long predicted the intrabinary interaction and related high-energy emission from black widows (e.g., Arons & Tavani 1993). Studies of the γ -ray emission from the intrabinary region allow us to explore the detailed physical processes within such a binary (e.g., Roberts et al. 2014). In this paper we report the detection of orbitally modulated γ -ray emission from a recently discovered black widow PSR J1311–3430, which thus indicates the intrabinary origin for part of its emission.

PSR J1311–3430 was initially listed as an unassociated source in the *Fermi* Large Area Telescope (LAT) source catalog (2FGL J1311.7–3429; Nolan et al. 2012). It is the only γ -ray selected MSP with γ -ray pulsed emission discovered via a direct blind search in the *Fermi* data (Pletsch et al. 2012). The pulsed radio emission soon was detected too (Ray et al. 2013), but the signal was visible only during $<10\%$ of the observation time, suggesting strong variations in the intrabinary medium. Before the discovery, the source was found to have orbital modulation with a short period of $\simeq 94$ minutes through optical imaging and spectroscopy (Romani 2012; Romani et al. 2012). Considering its properties of weak X-ray emission, sinusoid-like optical modulation and large modulation amplitude, it was already suggested to be a black widow system and the optical modulation is caused by irradiation of the companion by the pulsar wind (Romani 2012). Marginal modulated X-ray emission possibly related to the intrabinary shock has also been detected (Romani 2012; Kataoka et al. 2012). The γ -ray discovery of the 2.56 ms spin signal thus confirmed its black widow nature (Pletsch et al. 2012). Analyzing the *Fermi* data, we searched and found the orbital modulation signal from the source’s offpulse emission. Below we present the data analysis and results in Section 2. The results

are discussed in Section 3.

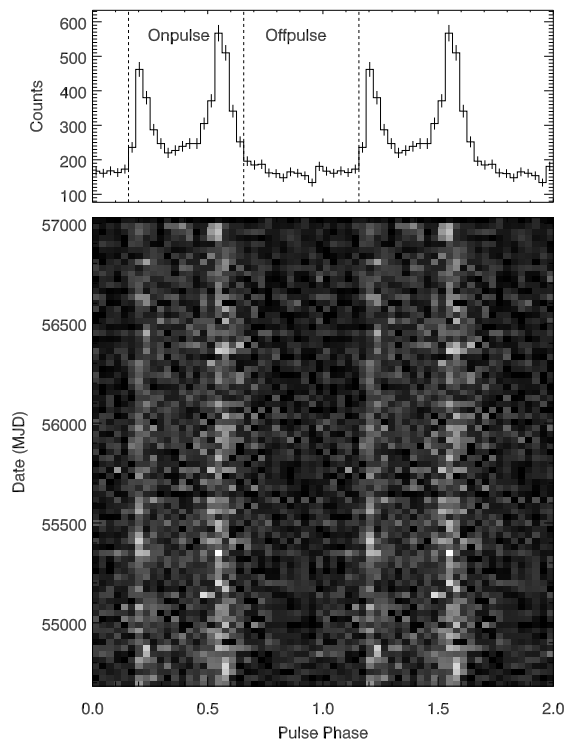


FIG. 1.— Folded pulse profile and two-dimensional phaseogram in 32 phase bins obtained for PSR J1311–3430. The gray scale represents the number of photons in each bin, and the dashed lines mark the onpulse and offpulse phase intervals.

2. DATA ANALYSIS AND RESULTS

2.1. *Fermi* LAT data

We selected 0.1–300 GeV LAT events from the *Fermi* Pass 7 Reprocessed (P7REP) database inside a $20^\circ \times 20^\circ$ region centered at the position of PSR J1311–3430 (Pletsch et al. 2012) during the time period from 2008-08-04 15:43:36 to 2015-01-06 21:19:57 (UTC). Only events with zenith angle less than 100° and during good time intervals were kept. The former prevents the Earth’s limb contamination, and for the latter, the quality of the data was not affected by the spacecraft events.

2.2. Timing Analysis

We performed timing analysis to the 0.1–300 GeV LAT data of the PSR J1311–3430 region to update the γ -ray ephemeris given in Pletsch et al. (2012). An aperture radius of 1.0° was used. We determined the pulse time of arrivals (TOAs) by obtaining the pulse profiles of 40 evenly divided segments using the known ephemeris (Pletsch et al. 2012) and cross-correlated them with a template profile created with data during the time period of MJD 54682–56119 (the same time range as that in Pletsch et al. 2012), following the algorithm described in Taylor (1992). We used TEMPO2 (Hobbs et al. 2006; Edwards et al. 2006) to fit the TOAs. Only pulse frequency f and frequency derivative \dot{f} were fitted, and the other timing parameters were fixed to their known values. We obtained $f = 390.56839326403(7)$ Hz and $\dot{f} = -3.193(1) \times 10^{-15} \text{ s}^{-2}$, consistent with the values

given in Pletsch et al. (2012) within $\sim 0.5\sigma$ and $\sim 2.2\sigma$ uncertainties, respectively. The folded pulse profile and two-dimensional phaseogram are shown in Figure 1. We defined phase 0.16–0.66 and 0.66–1.16 as the onpulse and offpulse phase intervals, respectively.

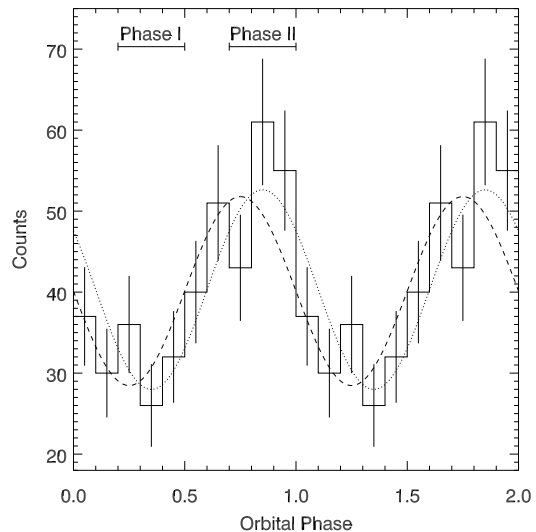


FIG. 2.— 0.2–300 GeV light curve folded at the orbital period using the offpulse data. The bottom (Phase I) and peak (Phase II) ranges of the modulation are marked. Two simple sinusoid fits are displayed as dashed and dotted curves; for the latter, 0.1 phase shift is forced (see the text in Discussion).

2.3. Maximum Likelihood Analysis

We selected LAT events in 0.1–300 GeV energy range for the likelihood analysis, and included all sources within 20° in the *Fermi* third source catalog (The *Fermi*-LAT Collaboration 2015) centered at the position of PSR J1311–3430 to make the source model. The spectral function forms of the sources are provided in the catalog. The spectral parameters of the sources within 5° from PSR J1311–3430 were set free, and all other parameters of the sources were fixed at their catalog values. The γ -ray counterpart of PSR J1311–3430 was modeled with an exponentially cutoff power law, characteristic for pulsars (Abdo et al. 2013), and a simple power law for comparison. In addition, we used the spectrum model `gll_iem_v05_rev1.fits` and the spectrum file `iso_source_v05.txt` to consider the Galactic and extragalactic diffuse emission, respectively.

Using the LAT science tools software package `v9r33p0`, we performed standard binned likelihood analysis to the LAT data. The γ -ray emission during the total pulse phase interval was detected with a Test Statistic (TS) value of 6279, while that during the onpulse and offpulse phase intervals were detected with TS values of 7723 and 499, respectively. The TS value at a specific position is calculated from $\text{TS} = -2 \log(L_0/L_1)$, where L_0 and L_1 are the maximum likelihood values for a model without and with an additional source respectively, and approximately is the square of the detection significance for the additional source (Abdo et al. 2010). We found during the total pulse phase, onpulse phase, and offpulse phase intervals, the emission is better modeled by an exponentially cutoff power law, with the low energy cutoff detected with $>13\sigma$, $>14\sigma$, and $>5\sigma$ significance (esti-

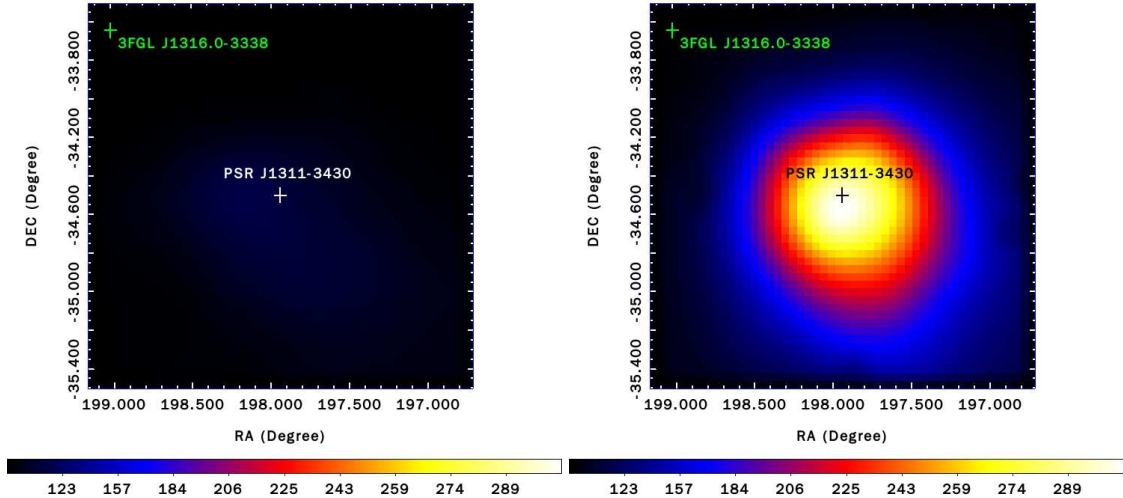


FIG. 3.— 0.2–300 GeV TS maps of a $2^\circ \times 2^\circ$ region centered at the position of PSR J1311–3430 during Phase I (*left*) and Phase II (*right*). The image scale of the maps is $0.04^\circ \text{ pixel}^{-1}$. The color bars indicate the TS value range. All sources in the source model except PSR J1311–3430 were considered and removed. The white (*left*) and dark (*right*) crosses mark the position of PSR J1311–3430, and the green cross marks the position of the nearby catalog source 3FGL J1316.0–3338.

mated from $\sqrt{-2 \log(L_{pl}/L_{exp})}$, where L_{exp} and L_{pl} are the maximum likelihood values for the exponentially cutoff power-law model and power-law model, respectively; Abdo et al. 2013). The resulting exponentially cutoff power-law fits are summarized in Table 1.

2.4. Orbital Variability

We folded the LAT events of the PSR J1311–3430 region at its orbital period (Pletsch et al. 2012) to study its possible orbital modulations. The source position given in Pletsch et al. (2012) was used for the barycentric corrections to photon arrival times, and photons within R_{max} (R_{max} ranges from 0.1° – 1.0° with a step of 0.1°) from the position were collected. Different energy ranges (0.1–300, 0.2–300, 0.3–300, 0.5–300, 1–300 GeV) were tested in folding. No significant modulations were detected using the whole data (i.e., during the total pulse phase), as the largest H-test value was 6 (corresponding to $<2\sigma$ detection significance; de Jager et al. 1989). However, a significant orbital signal was best revealed using the offpulse data in the >0.2 GeV energy range within 0.4° from PSR J1311–3430. The folded light curve, which has an H-test value of ~ 22 (corresponding to $\sim 4\sigma$ significance and $\sim 3\sigma$ post-trial significance, for the latter where 50 trials on the energy range and aperture radius are considered), is shown in Figure 2. The phase zero is at the ascending node of the pulsar (Pletsch et al. 2012). The folded light curve has a brightness peak around the superior conjunction (when the companion is behind the pulsar), the same as the modest X-ray one reported in Romani (2012). The similarity helps strengthen the γ -ray modulation detection. Using the LAT tool `gtexposure`, we checked the summed exposures over the 10 orbital phase bins (e.g., Johnson et al. 2015), and they had only $<1\%$ differences, too small to cause any artificial orbital modulations.

We performed likelihood analysis to the >0.2 GeV offpulse LAT events during the orbital phase ranges of 0.2–0.5 (named Phase I) and 0.7–1.0 (named Phase II), which were approximately defined for the bottom and peak of the orbital modulation, respectively. We found that the

emission during the both phase ranges is better modeled by an exponentially cutoff power law, with low energy cutoff detected with $>3\sigma$ and $>2\sigma$ significance. The exponentially cutoff power-law fits are summarized in Table 1. The TS values during Phase I and II are ~ 120 and ~ 320 (see Figure 3), respectively, which indicate that the source during the latter is more significantly detected than during the former, confirming the detection of orbital modulation from photon folding.

Possible contamination from a nearby catalog source 3FGL J1316.0–3338, which is identified as the counterpart to the flat spectrum radio quasar (FSRQ) PKS 1313–333 (Ackerman et al. 2015), was investigated. This source, being only $\sim 1.2^\circ$ away from PSR J1311–3430 and relatively bright (TS $\simeq 625$ in the catalog), exhibited flaring events in the past¹. Using the offpulse data and performing likelihood analysis, we extracted its 30-day interval light curve, and found that for five time bins (MJD 54863–54923, MJD 55433–55493, MJD 56363–56393), it had fluxes $>2\sigma$ above the value obtained from the total offpulse data. We repeated the analysis by excluding the data of the time bins. We found that the folded light curve is nearly the same, still having an H-test value of $\simeq 22$.

2.5. Spectral Analysis

We further investigated the orbital-dependent spectral variability during the offpulse phase interval. Spectra of PSR J1311–3430 during the whole offpulse phase interval, Phase I, and Phase II were obtained, and the spectrum during the onpulse phase interval was also obtained for comparison. We extracted the spectra by performing maximum likelihood analysis to the LAT data in 10 evenly divided energy bins in logarithm from 0.1–300 GeV, with the emission of the source being modeled with a power law in each energy bin. We only kept spectral points with $TS \geq 4$, and derived the 95% upper limits in other energy bins. The spectra extracted by this method

¹ http://fermi.gsfc.nasa.gov/ssc/data/access/lat/4yr_catalog/ap_lcs.php

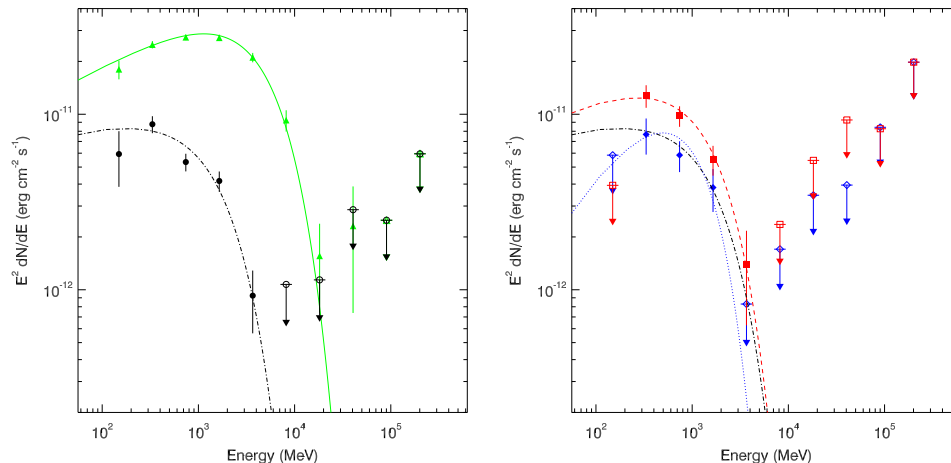


FIG. 4.— *Left panel:* γ -ray spectra of PSR J1311–3430 obtained with the onpulse (green triangles) and offpulse data (dark circles). *Right panel:* γ -ray spectra of PSR J1311–3430 obtained during offpulse Phase I (blue diamonds) and Phase II (red squares). The exponentially cutoff power-law fits for the onpulse and offpulse data are shown as green solid and dark dot-dashed curves, respectively. The same model fits for the offpulse Phase I and Phase II data are shown as blue dotted and red dashed curves, respectively.

are less model-dependent and provide a detailed description of the γ -ray emission for the source.

The obtained spectra are shown in Figure 4. The onpulse emission appears to have a 3-times higher cutoff energy E_c than the offpulse one (see also Table 1). In addition, comparing the two offpulse spectra, the source was brighter across the >0.2 GeV energy range during Phase II than during Phase I.

We also repeated the analysis by excluding the data when the nearby source 3FGL J1316.0–3338 had possible flares (see § 2.4). The obtained spectral parameters of PSR J1311–3430 during the two orbital-phase ranges are consistent with the values obtained above (within 1σ uncertainties). We concluded that the flares do not have any significant effect on our spectral analysis. However, we note that in the lowest energy bin, the two upper limits of the Phase I and II spectra (see the right panel of Figure 4) are lower than the exponentially cutoff power-law fits. This problem might be due to possible contamination from 3FGL J1316.0–3338 in the low-energy range.

3. DISCUSSION

From our analysis of the *Fermi* data of PSR J1311–3430, we have detected its γ -ray orbital modulation during the offpulse phase interval of the pulsar, where the magnetospheric emission from the pulsar was likely effectively removed. In both optical and X-ray observations, flares were detected (Romani 2012), indicating the strong interaction between the pulsar wind and the companion. Likely γ -rays are also produced due to the intrabinary interaction. However, different from that is seen in PSR B1957+20, which has an extra component above 2.7 GeV at its inferior conjunction (when the companion is in front of the pulsar), the light curve peak is near the superior conjunction for PSR J1311–3430. The difference suggests that the intrabinary γ -ray emission model, which explains the extra component as the result from viewing an inverse Compton process as a head-on collision (see also Bednarek (2014)), proposed in Wu et al. (2012) does not apply here.

For PSR J1311–3430, no significant spectral changes were found from the offpulse orbital-phase-resolved spec-

tra (Figure 4). The source appeared brighter across the >0.2 GeV energy range during the peak range (Phase II) than during the bottom range (Phase I). Although the uncertainties from our fits with the exponentially cutoff power law are relatively large, the two spectra are generally similar to each other. The similarity suggests an geometric origin for the orbital modulation, such as that used to explain the X-ray orbital modulation of PSR J1023+0038 (Bogdanov et al. 2011). The binary likely has an inclination angle of $i \sim 60^\circ$, and the companion has a very small Roche lobe radius $R_L = 0.068 R_\odot$ (a canonical neutron star mass $M_n = 1.35 M_\odot$ is assumed). Therefore like in PSR J1023+0038, the intrabinary emission region must be very close to the companion and the companion can thus block part of the region, causing the observed orbital modulation. Here we simply assume that the region is at the inner surface of the companion, and use a function $m_h[1 + \sin(2\pi\phi - \pi)\sin i]/2 + m_c$ to describe the orbital modulation, where ϕ is the orbital phase, $i = 60^\circ$ is fixed, and m_h and m_c are the modulation amplitude (in units of counts) and constant counts, respectively. Fitting the folded light curve, we found this function can describe the modulation (see Figure 2), where the minimum $\chi^2 = 9.7$ (for 8 degrees of freedom) and $m_h = 27 \pm 7$, $m_c = 27 \pm 3$. However, examining the light curve, the minimum and maximum may have a 0.1 phase shift (i.e., they occur at phase 0.35 and 0.85, respectively). If we force such a shift, the results are $\chi^2 = 7.9$ (for 8 degrees of freedom) and $m_h = 28 \pm 7$, $m_c = 26 \pm 3$, indeed slightly better. This shift may suggest that the emission is not isotropic. The constant part m_c may represent the intrabinary emission unblocked by the companion over the whole orbital phase, while emission from the pulsar during its offpulse phase interval could also contribute a small fraction.

It is not clear why PSR J1311–3430 has an orbital modulation different from that of PSR B1957+20. We note that if the size of the interaction region is proportional to that of a companion, similar fractions of an isotropic pulsar wind (0.0021 vs. 0.0024) would be intercepted for PSR J1311–3430 and PSR B1957+20 respectively (estimated from $(R_2/D_b)^2/4$; R_2 is the radius

TABLE 1
EXPONENTIALLY CUTOFF POWER-LAW FITS FOR PSR J1311–3430.

Data set	>0.1 GeV Flux (10^{-8} photon $\text{cm}^{-2} \text{s}^{-1}$)	Γ	E_c (GeV)	TS
Total data	8.9 ± 0.4	1.80 ± 0.04	4.0 ± 0.5	6279
Onpulse data	13.9 ± 0.6	1.71 ± 0.04	3.9 ± 0.4	7723
Offpulse data	4.6 ± 0.6	1.9 ± 0.2	1.3 ± 0.4	499
Offpulse Phase I	3 ± 1	1.2 ± 0.7	0.6 ± 0.3	120
Offpulse Phase II	7 ± 2	1.8 ± 0.5	1.2 ± 0.9	320

NOTE. — Column 3 and 4 list the photon index and cutoff energy of the exponentially cutoff power-law model.

of the companion and D_b is the separation distance of the binary). The notable differences are that the spin-down luminosity of PSR J1311–3430 is approximately 1/3 of PSR B1957+20 and that the companion in PSR J1311–3430 nearly fills its Roche lobe (Romani et al. 2012). We suspect that because of the latter, an outflow from the companion may still exist, the same as that in PSR J1023+0038 (e.g., Bogdanov et al. 2011). For PSR B1957+20, its companion fills its Roche lobe $\sim 85\%$ (Reynolds et al. 2007), and the mass loss from the companion is presumably driven by the pulsar wind (Arons & Tavani 1993 and references therein). The much more messy environment in PSR J1311–3430, as suggested by the radio observations (Ray et al. 2013), could be evidence for this possibility. Detailed modeling for physical processes in PSR J1311–3430 would help verify it.

Our discovery of the orbital γ -ray modulation in PSR J1311–3430 and the analysis results have provided clear evidence for γ -ray production due to intrabinary interaction between a pulsar and its companion in a black widow system, and thus have confirmed the general phys-

ical picture that has long been proposed theoretically. Since X-ray observations have revealed the general existence of intrabinary shock emission in eclipsing MSP binaries, similar work can be carried out to search and study related γ -ray emission from these recently identified systems.

We thank the anonymous referee for helpful suggestions. This research made use of the High Performance Computing Resource in the Core Facility for Advanced Research Computing at Shanghai Astronomical Observatory. This research was supported by the Shanghai Natural Science Foundation for Youth (13ZR1464400), the National Natural Science Foundation of China for Youth (11403075), the National Natural Science Foundation of China (11373055), and the Strategic Priority Research Program “The Emergence of Cosmological Structures” of the Chinese Academy of Sciences (Grant No. XDB09000000). Z.W. is a Research Fellow of the One-Hundred-Talents project of Chinese Academy of Sciences.

REFERENCES

- Abdo, A. A., et al. 2010, *ApJS*, 188, 405
—, 2013, *ApJS*, 208, 17
Ackerman, M., Ajello, M., Atwood, W., et al. 2015, *arXiv:1501.06054*
Alpar, M. A., Cheng, A. F., Ruderman, M. A., & Shaham, J. 1982, *Nature*, 300, 728
Archibald, A. M., Kaspi, V. M., Bogdanov, S., Hessels, J. W. T., Stairs, I. H., Ransom, S. M., & McLaughlin, M. A. 2010, *ApJ*, 722, 88
Arons, J., & Tavani, M. 1993, *ApJ*, 403, 249
Bednarek, W. 2014, *A&A*, 561, A116
Bogdanov, S., Archibald, A. M., Hessels, J. W. T., Kaspi, V. M., Lorimer, D., McLaughlin, M. A., Ransom, S. M., & Stairs, I. H. 2011, *ApJ*, 742, 97
Bogdanov, S., Patruno, A., Archibald, A. M., Bassa, C., Hessels, J. W. T., Janssen, G. H., & Stappers, B. W. 2014, *ApJ*, 789, 40
de Jager, O. C., Raubenheimer, B. C., & Swanepoel, J. W. H. 1989, *A&A*, 221, 180
Edwards, R. T., Hobbs, G. B., & Manchester, R. N. 2006, *MNRAS*, 372, 1549
Fruchter, A. S., Stinebring, D. R., & Taylor, J. H. 1988, *Nature*, 333, 237
Gentile, P. A., et al. 2014, *ApJ*, 783, 69
Hobbs, G. B., Edwards, R. T., & Manchester, R. N. 2006, *MNRAS*, 369, 655
Huang, R. H. H., Kong, A. K. H., Takata, J., Hui, C. Y., Lin, L. C. C., & Cheng, K. S. 2012, *ApJ*, 760, 92
Kataoka, J., et al. 2012, *ApJ*, 757, 176
Manchester, R. N., Hobbs, G. B., Teoh, A., & Hobbs, M. 2005, *AJ*, 129, 1993
Nolan, P. L., et al. 2012, *ApJS*, 199, 31
Pletsch, H. J., et al. 2012, *Science*, 338, 1314
Radhakrishnan, V., & Srinivasan, G. 1982, *Current Science*, 51, 1096
Ray, P. S., et al. 2013, *ApJ*, 763, L13
Reynolds, M. T., Callanan, P. J., Fruchter, A. S., Torres, M. A. P., Beer, M. E., & Gibbons, R. A. 2007, *MNRAS*, 379, 1117
Roberts, M. S. E. 2013, in *IAU Symposium*, Vol. 291, IAU Symposium, ed. J. van Leeuwen, 127–132
Roberts, M. S. E., McLaughlin, M. A., Gentile, P., Aliu, E., Hessels, J. W. T., Ransom, S. M., & Ray, P. S. 2014, *Astronomische Nachrichten*, 335, 313
Romani, R. W. 2012, *ApJ*, 754, L25
Romani, R. W., Filippenko, A. V., Silverman, J. M., Cenko, S. B., Greiner, J., Rau, A., Elliott, J., & Pletsch, H. J. 2012, *ApJ*, 760, L36
Johnson, T. J., Ray, P. S., Roy, J., Cheung, C. C., Harding, A. K., Pletsch, H. J., Fort, S., Camilo, F., Deneva, J., Bhattacharyya, B., Stappers, B. W. 2015, *arXiv:1502.06862*
Taylor, J. H. 1992, *Royal Society of London Philosophical Transactions Series A*, 341, 117
The Fermi-LAT Collaboration. 2015, *ArXiv e-prints*
Wu, E. M. H., Takata, J., Cheng, K. S., Huang, R. H. H., Hui, C. Y., Kong, A. K. H., Tam, P. H. T., & Wu, J. H. K. 2012, *ApJ*, 761, 181
Xing, Y., & Wang, Z. 2014, *ArXiv e-prints*
Xing, Y., Wang, Z., & Ng, C.-Y. 2014, *ApJ*, 795, 88